

# Advanced simulation of the earth-to-air heat exchangers – a comparison between simulation and measured data

Pavel Kopecký, Jan Tywoniak,  
Czech Technical University in Prague, Faculty of Civil Engineering, Department of Building Structures, Czech Republic  
[pavel.kopecky@fsv.cvut.cz](mailto:pavel.kopecky@fsv.cvut.cz)

## Abstract

*The paper deals with the earth-to-air heat exchanger (EAHX) simulation and monitoring. A newly developed hygro-thermal model for transient simulation of EAHXs has already been validated against an analytical solution; a comparison with performance data of real EAHXs has missed so far. The model is tested against long-term monitoring of two simple earth-to-air heat exchangers connected with mechanical ventilation in two low-energy family houses. In parallel, the differential sensitivity analysis is used for a model assessment. The comparison between measured data and numerical simulation does not correlate absolutely. However, the simulation is capable to show limitations and energy saving potential of the exchanger with respect to building ventilation. The model brings clear information about processes which take place during earth-to-air heat exchanger operation.*

## 1. Introduction

The earth-to-air heat exchanger (EAHX) is a pipe buried in the ground through which air is sucked into a building. Either the computer simulation or monitoring of real size EAHXs is a way to study hygro-thermal performance of EAHXs. The performance depends on (without order) the air flow rate, convective heat transfer between flowing air and internal pipe surface, heat exchange surface area (it depends on diameter, length and number of pipes), the soil temperature (it depends on the soil properties, depth, annual soil surface temperature profile, and previous operation of EAHX), inlet air temperature and relative humidity of the inlet air.

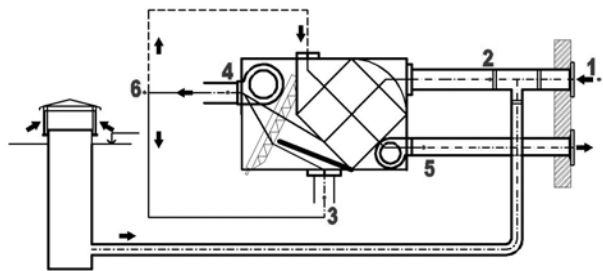
We use a model for simulation of EAHXs which was recently developed at the Czech Technical University in Prague. The model deals with heat balance of air inside pipes including latent heat of possible condensation and/or evaporation and with transient heat conduction around pipes when a special attention is paid to the upper soil surface boundary. The calculation routine has been developed within MATLAB environment and is represented by several inter connected functions. The theoretical basis of the model including developed algorithm and the analytical validation was presented in [1, 2].

## 2. Measurement in situ

### 2.1. Low-energy family house in Velké Popovice

The low-energy family house using mechanical ventilation equipped with heat recovery and a simple earth-to-air heat exchanger has been monitored since the end of summer 2004. The scheme of the system with placement of sensors is in Figure 1. Table 1 gives a basic description of EAHX. The monitoring had several imperfections. The interval of the measurement (20 min, later changed to 5 min) was too long, the air flow rate was not measured directly, and relative humidity of inlet and outlet air was not measured. Therefore, the ventilation mode (current state of the ventilation unit) was often difficult to figure out.

Despite these imperfections, several measurement data can be used for a comparison with the prediction.



1. Temperature of ambient air
2. Outlet air temperature
3. Temperature of circulation air
4. Temperature (circulation + fresh air)
5. Temperature of waste air (after heat recovery)
6. Internal air temperature (in staircase space)
7. Global solar radiation on horizontal plane

Figure 1: Velké Popovice – the monitored system with placement of sensors

Table 1: Description of evaluated EAHX

Number of pipes	Length of pipe [m]	Diameter [mm]	Depth [m]
1	21	200	2.0
Air flow rate [m <sup>3</sup> /h]	Soil	Control strategy	Place
100 – 350, higher values for summer ventilation	no data	According to $t_a$ and link to the actual mode of the ventilation unit	Velké Popovice, central Bohemia, near Prague

## 2.2. Passive family house in Rychnov

The passive family house ventilated by mechanical ventilation equipped with heat recovery and a simple earth-to-air heat exchanger is being monitored. The scheme of the ventilation system is in Figure 2. Table 2 gives a basic description of EAHX. The system allows the circulation of air between a ventilated zone and EAHX (option of cooling). The measurement is much more extensive than latter one. Measured data are collected in main data logger (measuring frequency 1 min) and two independent data loggers (measuring frequency 5 min). The first one is directly placed in the inlet shaft (position 2 in Figure 2); the second one is a living room data logger collecting data about temperature, relative humidity, and CO<sub>2</sub> concentration in internal air. The short step of measurement allows the accurate determination of the ventilation regime. Hence, it allows the precise determination of time intervals when EAHX was in operation and corresponding value of the air flow rate. The monitoring of air relative humidity also allows the determination whether air passing through the pipe was moistened (the deficit of moisture indicates condensation).

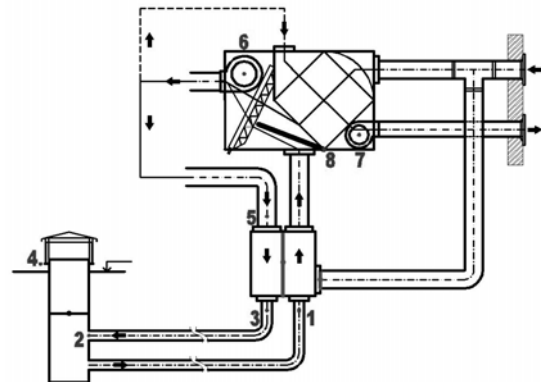


Figure 2: Rychnov – the monitored system with placement of sensors

1. Temperature + relative humidity [°C, %]
2. Temperature + relative humidity [°C, %]
3. Temperature + relative humidity [°C, %]
4. Ambient air temperature (on the facade and outside of the shaft) [°C]
5. Temperature (circulation air) [°C]
6. Air flow rate – suction fan [V, ac]
7. Air flow rate – exhaust fan [V, ac]
8. Flap position [V, dc]

Table 2: Description of evaluated EAHX

Number of pipes	Length of pipe [m]	Diameter [mm]	Depth [m]
2	23	200	1.0 and 2.0
Air flow rate [m <sup>3</sup> /h]	Soil	Control strategy	Place
115 – 410, higher values for summer ventilation	clay, homogenous	According to $t_a$ and link to the actual regime of the ventilation unit	Rychnov near Jablonec nad Nisou, North Bohemia

### 3. EAHX operation

EAHX operation pattern is important for understanding of time scales of thermal process. The pattern is rather important in order that a correct time step of the simulation should be chosen. Two months of EAHX operation based on the monitoring of the family house in Rychnov are depicted in Figure 3 (January 2006, pre-heating mode) and in Figure 4 (June 2006, cooling mode). The operation of EAHX in pre-heating mode was intermittent, as shown in Figure 3. The short horizontal stripes, visible especially in Figure 3, represent automatic cyclic ventilation of the house in the night. The EAHX operation visible near the noon is the ventilation induced by preparations of lunch. The operation in cooling mode was not as intermittent as in the pre-heating mode. It was concentrated on daytime during a hot spell (Figure 4).

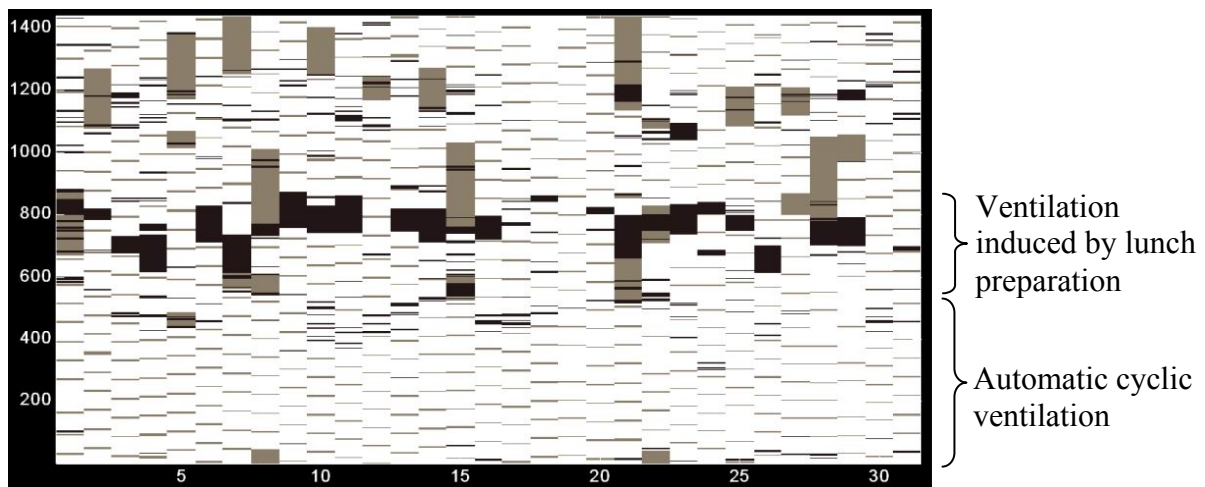


Figure 3: EAHX operation in Rychnov (January 2006), the vertical axis represents time during a day in minutes, the horizontal axis represents days, and grey tones represent the value of air flow rate (115 m<sup>3</sup>/h grey, 198 m<sup>3</sup>/h black)

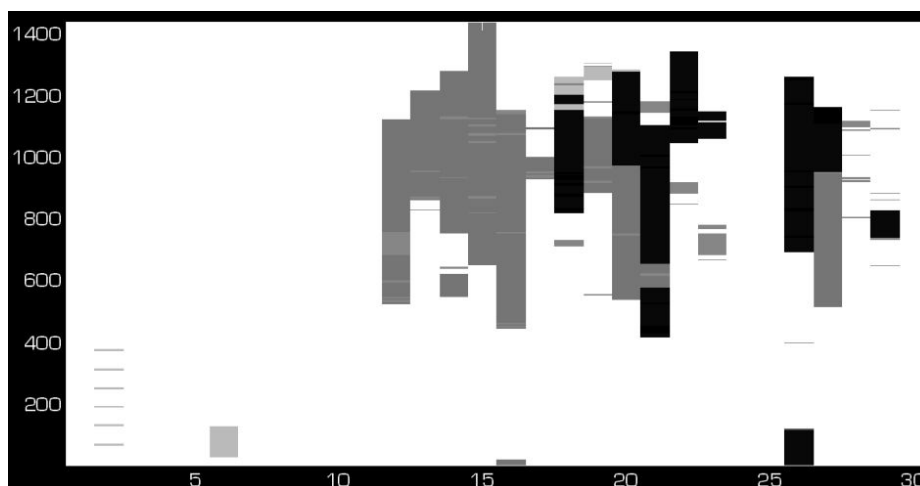


Figure 4: EAHX operation in Rychnov (June 2006), the vertical axis represents time during a day in minutes, the horizontal axis represents days, and grey tones represent the air flow rate (115, 198, 221 m<sup>3</sup>/h grey, 401 m<sup>3</sup>/h black)

The intermittency of the operation causes some problems to simulation. If one wanted to be correct, it would be necessary to use very short time step of the simulation (approximately 5 min for simulation of pre-heating mode). However, the shortest thermal pulse lasts a few minutes and the pulse is followed by soil thermal recovery which is much longer than the

pulse itself (see Figure 3). Therefore, the thermal impact on the surrounding soil of such pulses is negligible.

#### 4. Long-term simulation

EAHX in Velké Popovice was simulated. A calculation domain was a block 8 m (width) x 5 m (height) x  $L$  (length of the pipe). The domain was divided on 17 x 15 x 21 control volumes. The pipe was approximated by an equivalent square with perimeter which equals to the perimeter of the pipe. The upper edge of the equivalent square had distance  $Z_p$  from the upper side of the block (soil surface). The simulation was performed in schedules as shown in Table 3; the time step of the simulation was 1200 seconds. The influence of the inlet shaft was not simulated; the inlet air temperature was equal to ambient air temperature. The inlet air was assumed to be absolutely dry. A boundary condition for soil surface was set up by ambient air temperature, global solar radiation on a horizontal plane (assumed 80% absorptivity for solar radiation), convective surface thermal resistance (the influence of wind, assumed to be constant value  $0,04 \text{ m}^2\text{KW}^{-1}$ ) and inserted additional thermal resistance  $R_s$  representing the influence of soil cover (vegetation, snow, defined by user defined function). Strictly, the soil surface boundary condition should also contain many other factors. Perhaps except the long wave radiation between soil surface and surrounding surfaces, these factors only influence a few upper centimeters of soil, for they are based on daily time scale (e.g. morning condensation followed by evaporation). Therefore, it was possible to leave them out of balancing the upper soil surface boundary condition. Other walls of the rectangle were assumed to be adiabatic.

Table 3: The specification of the simulation

	start	finish						
	30.8. 2004	1.1.	25.2.	7.3.	25.5.	1.6.	25.7.	23.8. 2005
<b>Ini*</b>	125	125	125	0	350	0	350	0

\* **Ini** denotes the initiation of the simulation. The initiation period is the simulation of two years when no EAHX works. Thus, soil temperature field is only influenced by upper soil surface boundary; geothermal heat flow was omitted too. The main purpose of the initiation is to build up the undisturbed soil temperature field as accurately as possible. The vertically hatched field in Table 3 denotes the intermittent operation of EAHX; turned on when  $t_a = 0 \text{ }^\circ\text{C}$ , turned off when  $t_a = +5 \text{ }^\circ\text{C}$ . The number in the frame is the air flow rate in ( $\text{m}^3\text{h}^{-1}$ ). In reality, EAHX operation is not only the function of the ambient air temperature, but it also depends on the actual ventilation mode. The grey shaded field denotes the identical EAHX operation as monitored.

##### 4.1. Sensitivity analysis

Sensitivity analysis is the important part of the model validation. The analysis should help to identify input parameters to which the model outputs are particularly sensitive and to get parameters to which the outputs are not sensitive. It is especially important to identify sensitive input parameters with high uncertainty.

The method of Differential Sensitivity Analysis [3] was used in this paper. The method is based on varying just one input parameter for each simulation while remaining inputs stay fixed at their most likely base case values (BC). The change in predicted output parameter  $\Delta p_i$  represents an effect of uncertainty in  $i$  - th input parameter:

$$\Delta p_i = p_i - p_{BC} \quad (1)$$

Firstly, the sensitivity of the annual soil temperature amplitude  $t_z^A$  ( $^{\circ}\text{C}$ ) to uncertainty in input parameters (parameters 1 to 6 in Table 4) was studied. The soil temperature is monitored in the first soil control volume above the equivalent pipe during the second year of the initiation. Thus, such soil temperature represents undisturbed soil temperature during a year in depth closed to depth in which EAHX is placed. Next, the sensitivity of the total energy  $E_{EAHX}$  (kWh) injected to or extracted from soil during simulated period (30.8.2004 – 23.8.2005) to uncertainty in all input parameters (Table 4) was studied. The effect of spatial and time discretization was not studied in this paper. It is assumed the grid was generated dense enough to produce correct results.

Table 4: Uncertainties in input parameters

			<b>b</b>	<b>BC</b>	<b>a</b>	<b>note</b>	
1	$\lambda_s$	$[\text{Wm}^{-1}\text{K}^{-1}]$	-1.0	1.5	+1.0	range of common soils	
2	$\rho c_p$	$[\text{MJm}^{-3}\text{K}^{-1}]$	-1.5	3.0	+1.5	range of common soils	
3	$T_{in}$	$[^{\circ}\text{C}]$	-0.2	from measurement	+0.2	measurement uncertainty	
4	$I_g$	$[\text{Wm}^{-2}]$	-3%	from measurement	+3%	measurement uncertainty	
5	$R_s$	$[\text{m}^2\text{KW}^{-1}]$	-50%	UDF	+50%	UDF = user defined function, guess	
6	$Z_p$	$[\text{m}]$	-0.25	2.0	+0.25	pipe slope	
7	$L$	$[\text{m}]$	-3.0	21	+3.0	pipe length	
8	$V_a$	$[\text{m}^3\text{h}^{-1}]$	-25	125	+25	pre-heating	guess
			-50	350	+50	cooling	
9	$h_a$	$[\text{Wm}^{-2}\text{K}^{-1}]$	-25%	calculation from $Nu$	+25%	guess	

Table 5: Soil properties in simulation

	$\lambda_s$	$\rho$	$c_p$	$\rho c_p$	$a_s * 10^{-6}$	$b_s$
	$[\text{Wm}^{-1}\text{K}^{-1}]$	$[\text{kgm}^{-3}]$	$[\text{Jkg}^{-1}\text{K}^{-3}]$	$[\text{MJm}^{-3}\text{K}^{-1}]$	$[\text{m}^2\text{s}^{-1}]$	$[\text{Ws}^{0.5}\text{m}^{-2}\text{K}^{-1}]$
BC	1.5	2000	1500	3.0	0.50	2121
1a	2.5	2000	1500	3.0	0.83	2739
1b	0.5	2000	1500	3.0	0.17	1225
2a	1.5	2250	2000	4.5	0.33	2598
2b	1.5	1500	1000	1.5	1.00	1500

Soil temperature calculated during the initiation of simulations is depicted in Figure 5. The effect of input uncertainties monitored on the value of the soil amplitude ( $4.7^{\circ}\text{C}$  for BC) is given in Figure 6, left. Uncertainties assumed in soil properties (Table 5) have the strongest impact; the undisturbed soil temperature strongly depends on the value of the soil thermal diffusivity and the resulting upper soil surface temperature. The effect of input uncertainties monitored on the value of total energy injected to or extracted from the soil (451 kWh for BC) is given in Figure 6, right. Uncertainties assumed in soil properties, length of the pipe, depth of the pipe, air flow rate, and the convective heat transfer coefficient have the strongest impact on model performance.

The interesting detail is the performance of 1b case. Although the undisturbed soil temperature is the most stable in that case (the lowest value of soil thermal diffusivity), this particular advantage does not overweight poor thermal transport near the pipe. The performance of cases 2a and 1a needs another comment. Although the value of the soil thermal conductivity of case 2a is lower than in case 1a, case 2a shows the overall thermal performance better than case 1a. Both cases have similar soil thermal effusivity; however,

case 2a has the value of soil thermal diffusivity much lower than case 1a. Thus, the undisturbed soil temperature of case 2a is much more stable than in case 1a, and this particular advantage is the most decisive because both cases have similar value of thermal effusivity.

The slightly non-linear reaction of the model to uncertainties in the inlet air temperature is not caused by non-linear effects of the model. The temperature of inlet air is a parameter which governs whether EAHX is turned on, or turned off. As a result, we get different operation patterns for cases 3a, 3b and BC, and we consequently get different total energy extracted from or injected to the soil.

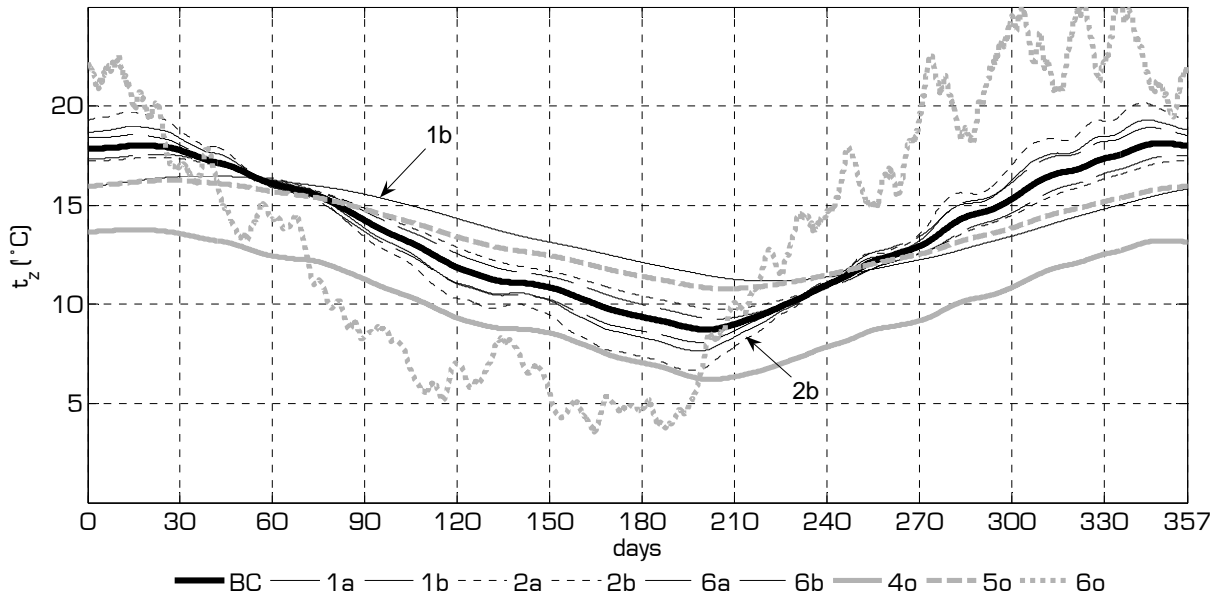


Figure 5: Soil temperatures  $t_z$  (°C) calculated during initiation of simulation; 4o is BC without solar radiation; 5o is BC with  $R_s$  assumed to be a constant value  $1.0 \text{ m}^2\text{KW}^{-1}$ ; 6o is BC with pipe depth 0.5 m

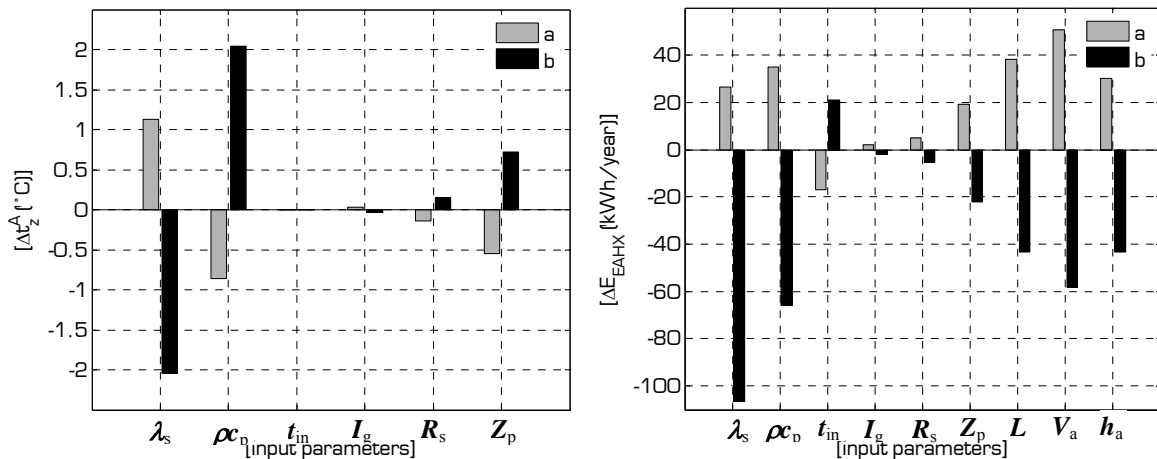


Figure 6: Effect of uncertainties in inputs – bar chart representation of sensitivity analysis results for annual soil temperature amplitude (left) and for total energy delivered to or extracted from the soil (right)

## 4.2. Comparison with measurement

Following time intervals were chosen so that we would compare simulations with measured data: a) 25.2. – 6.3.2005 and b) 25.7. – 31.7.2005. The first interval is the last term of air pre-heating during winter 2004/2005, and the second interval is the second hot spell of summer 2005 (air cooling). The comparison of measured outlet air temperature with simulated values

is in Figure 7 and in Figure 8. The results of variants with the most significant uncertainties are depicted too. They show us an interval in which all simulation results were found.

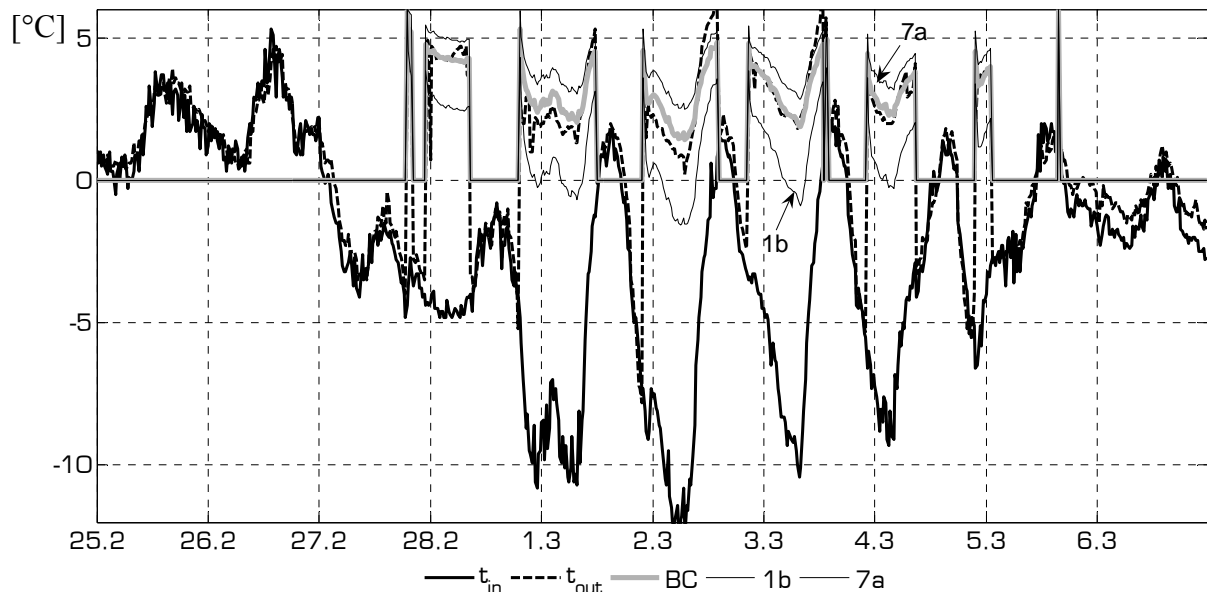


Figure 7: 25.2. – 6.3.2005; measured inlet ( $t_{in}$ ) and outlet ( $t_{out}$ ) air temperatures vs. simulated outlet air temperature

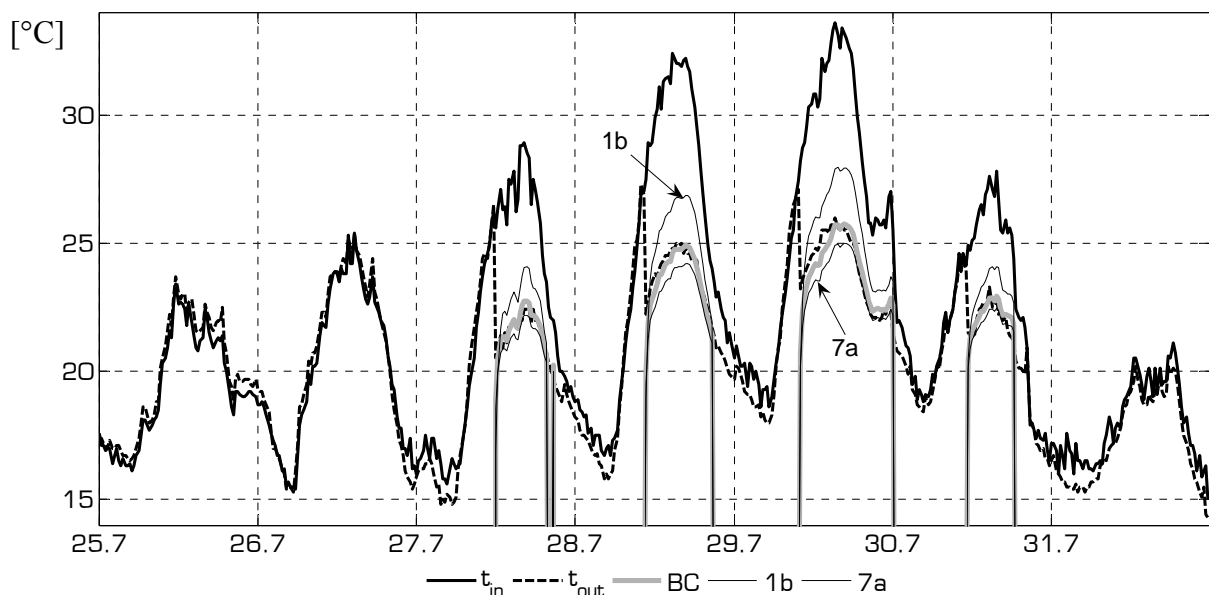


Figure 8: 25.7. – 31.7.2005; measured inlet ( $t_{in}$ ) and outlet ( $t_{out}$ ) air temperatures versus simulated outlet air temperature

## 6. Conclusion

On the basis of presented results following conclusions were formulated:

- The accurate simulation of EAHX is rather difficult because of small air-to-soil heat flows and the intermittent pattern of EAHX operation; the relative error of the model prediction can be high.
- The quality of the model prediction is rather dependent on the accurate estimation of the natural thermal stratification in soil during the initiation of the simulation. The operation of EAHX disturbs this natural stratification of the soil temperature.

- The accuracy of the numerical model was destroyed by uncertainties in several input parameters (primarily soil properties, the air flow rate, and the calculation of the convective heat transfer). Even more simplified models might be suitable for the simulation of EAHX, and perhaps they will not be so sensitive to input parameters uncertainties. However, the numerical model brings clear information about processes which take place during EAHX operation, and it allows a detailed analysis. A perfect fit between measured data and simulation results is not so important.
- We have achieved quite good accuracy of the numerical simulation, as shown in comparison with measured data on the real size EAHX in Velké Popovice. However, this test itself is not sufficient proof of the model. We would like to follow up with the comparison of the simulation with measured data from real size EAHX in Rychnov.

## Acknowledgement

This outcome has been achieved with the financial support of the Ministry of Education, Youth and Sports of the Czech Republic, project No. 1M0579, within activities of the CIDEAS research centre.

## References

- [1] Kopecký, P., Tywoniak, J. Hygro-thermal numerical simulation model for earth-to-air heat exchangers: validation process and the example of simulation. Proc. of 5th International Conference on Advanced Engineering Design. Prague, 2006. It is also available at <http://kopeckyp.wz.cz/files/pdf/PK-AED06.pdf>
- [2] Kopecký, P. Zemní výměník tepla: model a validace. Vytápění Větrání Instalace 4 (2006).
- [3] Lomas, J., Eppel, H. Sensitivity analysis techniques for building thermal simulation programs. Energy and Buildings 19 (1992).

## Nomenclature

$t_a$	ambient air temperature [°C]
$t_z$	soil temperature [°C]
$t_{in}$	inlet air temperature [°C]
$t_{out}$	outlet air temperature [°C]
$\lambda_s$	thermal conductivity of soil [ $\text{W}\cdot\text{m}^{-1}\cdot\text{K}^{-1}$ ]
$\rho c_p$	volumetric heat capacity of soil [ $\text{J}\cdot\text{m}^{-3}\cdot\text{K}^{-1}$ ]
$a_s$	thermal diffusivity of soil [ $\text{m}^2\cdot\text{s}^{-1}$ ]
$b_s$	thermal effusivity of soil [ $\text{W}\cdot\text{s}^{0.5}\cdot\text{m}^{-2}\cdot\text{K}^{-1}$ ]
$I_g$	global solar radiation on the horizontal plane [ $\text{W}\cdot\text{m}^{-2}$ ]
$R_s$	additional thermal resistance (between soil surface temperature and the first soil node temperature) [ $\text{m}^2\cdot\text{K}\cdot\text{W}^{-1}$ ]
$Z_p$	pipe depth [m]
$L$	pipe length [m]
$V_a$	air flow rate [ $\text{m}^3\cdot\text{h}^{-1}$ ]
$h_a$	convective heat transfer coefficient [ $\text{W}\cdot\text{m}^{-2}\cdot\text{K}^{-1}$ ]